Aust. J. Phys., 1984, **37**, 157–77

Modelling Reactive Gas Flows within Shock Tunnels

I. M. Vardavas

UV Physics Unit, Research School of Physical Sciences,
Australian National University, G.P.O. Box 4, Canberra, A.C.T. 2601.

Abstract

An iterative method is presented for modelling reactive gas flows within shock tunnels. The method overcomes both the problem of the stiffness of the chemical rate equations, which arises due to the greatly varying reaction rates, and the throat singularity in the velocity equation for subsonic–supersonic flow within a Laval nozzle. The effects of Coulomb interactions which depress the ionization potential of the ionic species can also be included because of the iterative nature of the method. The method computes the state of the gas both along the flow and within the reservoir or stagnation region. Sample computations are given for air, carbon dioxide and nitrogen for reservoir–nozzle gas flows and for flows behind normal shocks.

1. Introduction

In studies of chemical relaxation phenomena, within nozzle flows and flows behind normal shocks, the computation of the state of the gas is made difficult by the greatly varying reaction rates which render the chemical rate equations stiff and by the throat singularity in the velocity equation when viscosity is negligible. In order to overcome the stiffness problem numerous methods have been developed; amongst them are the works of Eschenroeder *et al.* (1962), Treanor (1966), Lordi *et al.* (1966), and Bailey (1969) which were specifically designed for shock tunnel flows. More general methods for solving stiff differential equations have been recently discussed by McRae *et al.* (1982), amongst which are the work of Gear (1971) and the extensions to his work by Hindmarsh and Byrne (1975). These methods were either designed for or are capable of solving the chemical rate equations along the flow but require a different method in order to obtain the reservoir conditions which initiate the flow, such as the free-energy minimization technique (Newman and Allison 1966).

The present work provides a simple and efficient iterative method specifically designed to solve both the reservoir and the flow conditions of the gas. The iterative nature of the method allows the velocity field within a Laval nozzle to be easily computed and has the added advantage of allowing such effects as the depression of the ionization potential of the ionic species due to Coulomb interactions to be incorporated into the model.

The method is applied to quasi-one-dimensional steady adiabatic inviscid flows within nozzles and behind normal shocks. The effects of conduction and radiation losses are thus not included and the vibrational modes of the molecular species are taken

0004-9506/84/020157$02.00

to be in equilibrium with the local translational temperature or frozen to some initial value. The method is described in Section 2 together with its convergence criteria, while the gasdynamic equations and Coulomb interactions are discussed in Section 3. In Section 4 sample computations are given for reservoir–nozzle flow, nozzle flow initiated by the stagnation region of a reflected-type shock tunnel (see e.g. Stalker 1967) and flow behind a normal shock. The computations are found to be in very good agreement with the results of Lordi *et al.* (1966) and Miller and Wilder (1976) for the reservoir conditions, Eschenroeder *et al.* (1962) for nozzle flow, and McIntosh (1971) for flow behind a normal shock. However, computations of a CO_2 nozzle flow initiated by a high enthalpy reservoir are found not to produce the sharp inflection point in the CO_2 concentration that was found by Ebrahim and Hornung (1973). Such an inflection would be rather difficult to reconcile with the generally smooth variation of all the other species concentrations and gas properties in such a CO_2 flow.

2. Solution of Chemical Rate Equations

(*a*) *Iterative Method*

For a steady one-dimensional gas flow with velocity u ($\mathrm{cm\,s^{-1}}$) and density ρ ($\mathrm{g\,cm^{-3}}$) at a point x (cm) consisting of a total I of chemically reacting species X_i involved in a total J of reactions j, the rate equation for a species X_i in terms of the concentration q_i ($\mathrm{mol\,g^{-1}}$ of mixture) can be written as

$$u\frac{\mathrm{d}q_i}{\mathrm{d}x} = \left(\frac{\partial q_i}{\partial t}\right)_{\mathrm{chem}} = \frac{1}{\rho}\left(\frac{\partial \xi_i}{\partial t}\right)_{\mathrm{chem}}, \tag{1}$$

where $q_i = \xi_i/\rho$ and ξ_i is the concentration in $\mathrm{mol\,cm^{-3}}$. If $k_{\mathrm{f}j}(T)$ denotes the forward reaction rate at temperature T and $K_{\mathrm{c}j}(T)$ is the associated equilibrium constant then we have

$$\left(\frac{\partial \xi_i}{\partial t}\right)_{\mathrm{chem}} = \sum_{j=1}^{J} \psi_{ij}\, k_{\mathrm{f}j}\left(\prod_{l=1}^{I} \xi_l^{\nu_{lj}} - \frac{1}{K_{\mathrm{c}j}} \prod_{l=1}^{I} \xi_l^{\nu'_{lj}}\right), \tag{2}$$

and the right-hand side is of the functional form $F_i(\xi_1, \xi_2, ..., \xi_I; T)$. The coefficients ψ_{ij} are defined by $\psi_{ij} = \nu'_{ij} - \nu_{ij}$, where ν_{ij} and ν'_{ij} are the reactant and product stoichiometric coefficients respectively, defined by the reaction

$$\sum_{i=1}^{I} \nu_{ij} X_i \leftrightarrow \sum_{i=1}^{I} \nu'_{ij} X_i. \tag{3}$$

Equation (1) can then be written in the functional form

$$u\,\mathrm{d}q_i/\mathrm{d}x - G_i(q_1, q_2, ..., q_I; T, \rho) = 0, \tag{4}$$

where $G_i = F_i/\rho$. Now if a single reaction j goes to equilibrium, i.e. $k_{\mathrm{f}j} \gg 1$, then $|G_i| \gg |u\,\mathrm{d}q_i/\mathrm{d}x|$ and the rate equation (4) reduces essentially to the algebraic form $G_i = 0$. On the other hand, if all the reactions are frozen then $|G_i| \ll |u\,\mathrm{d}q_i/\mathrm{d}x|$ and we need to solve $u\,\mathrm{d}q_i/\mathrm{d}x = 0$. Apart from the rate equations we must also solve the atomic species concentration equations and these take the form

$$\sum_{i=1}^{I} \alpha_{ki} q_i = C_k, \tag{5}$$

where we have K such equations, one for each atomic species k. Here C_k is the number of atoms of element k per g of gas which is independent of the state of the flow and α_{ki} is the number of atoms of element k in species i. Thus, in order to obtain the total I of species concentrations q_i at any point in the flow we need to solve $I-K$ rate equations of the form (4) and K conservation equations of the form (5). In general this set of equations must be solved simultaneously with the gasdynamic conservation equations in order that T, ρ and u are consistent with the q_i at each point in the flow. For clarity we shall assume for the present that T, ρ and u are given.

Let us first define the vector $\boldsymbol{q}_n$ given by

$$\boldsymbol{q}_n = (q_{1n}, q_{2n}, \ldots, q_{In}),$$

representing all the species concentrations at some position x_n along the flow. For a sufficiently small step size in x we may rewrite (4) as

$$(q_{in} - q_{in-1})/\Delta t_n - G_i(\boldsymbol{q}_n) = 0, \tag{6}$$

where $\Delta t_n = (x_n - x_{n-1})/u_n$. We thus have a system of $I-K$ equations of the form (6) and K equations of the form (5). To solve this system at x_n, knowing $\boldsymbol{q}_{n-1}$ at x_{n-1}, we make an initial guess $\boldsymbol{q}_n^{(1)}$ for the species at x_n such that we introduce a set of errors $\boldsymbol{\varepsilon}_n^{(1)}$ defined by

$$(q_{in}^{(1)} - q_{in-1})/\Delta t_n - G_i(\boldsymbol{q}_n^{(1)}) = \varepsilon_{in}^{(1)}, \tag{7}$$

where $\boldsymbol{\varepsilon}_n$ has elements ε_{in}. Similarly we may write (5) as

$$\sum_{i=1}^{I} \alpha_{ki} q_{in}^{(1)} - C_k = \varepsilon_{kn}^{(1)}. \tag{8}$$

We then proceed to reduce the errors $\boldsymbol{\varepsilon}_n$ by obtaining a set of corrections $\bar{\boldsymbol{q}}_n^{(1)}$ which give the better estimate $\boldsymbol{q}_n^{(2)} = \boldsymbol{q}_n^{(1)} + \bar{\boldsymbol{q}}_n^{(1)}$. In order to obtain the vector $\bar{\boldsymbol{q}}_n^{(1)}$ we assume that $\boldsymbol{q}_n^{(2)}$ satisfies the system of equations (5) and (6) exactly and we make a first-order Taylor expansion of G_i about the $\boldsymbol{q}_n^{(1)}$ so that

$$G_i(\boldsymbol{q}_n^{(2)}) = G_i(\boldsymbol{q}_n^{(1)}) + \sum_{l=1}^{I} \bar{q}_{ln}^{(1)} \partial G_i(\boldsymbol{q}_n^{(1)})/\partial q_{ln}. \tag{9}$$

Thus, the first set of corrections $\bar{\boldsymbol{q}}_n^{(1)}$ are obtained by solving

$$\frac{\bar{q}_{in}^{(1)}}{\Delta t_n} - \sum_{l=1}^{I} \bar{q}_{ln}^{(1)} \frac{\partial G_i(\boldsymbol{q}_n^{(1)})}{\partial q_{ln}} = \varepsilon_{in}^{(1)} \tag{10}$$

for $i = 1, 2, \ldots, I-K$, and

$$\sum_{l=1}^{I} \alpha_{kl} \bar{q}_{ln}^{(1)} = -\varepsilon_{kn}^{(1)} \tag{11}$$

for $k = I-K+1, \ldots, I$. Thus, we need to solve the system

$$\mathbf{A}_n^{(1)} \bar{\boldsymbol{q}}_n^{(1)} = -\boldsymbol{\varepsilon}_n^{(1)}, \tag{12}$$

where $\mathbf{A}_n$ is the modified Jacobian matrix with elements

$$a_{iln} = 1/\Delta t_n + 1/\tau_{iln}, \qquad \text{for } i = l \text{ and } i \leqslant I-K \tag{13a}$$

$$= 1/\tau_{iln}, \qquad \text{for } i \neq l \text{ and } i \leqslant I-K \tag{13b}$$

$$= \alpha_{il}, \qquad \text{for } i > I-K, \tag{13c}$$

and τ_{iln} is given by

$$1/\tau_{iln} = -\partial G_i/\partial q_{ln}, \tag{14}$$

where τ_{iln} can be thought of as a kind of characteristic time for the change in q_{in} due to a change in q_{ln}. The system of coupled linear stiff equations (12) can be ill-conditioned given great differences in the chemical reaction rates; however, this problem can be overcome by solving the system of equations using double precision gaussian elimination. Further, one could also incorporate partial pivoting and scaling of the Jacobian matrix (see e.g. Williams 1973) for better accuracy, but it should be remembered that the solution of the system of equations (12) only gives the Newton–Raphson corrections to the chemical species concentrations. Once the first corrections are found and $\boldsymbol{q}_n^{(2)}$ obtained the inversion is repeated until all the ε_{in} (equation 7) are sufficiently small. A good condition for convergence is that for all i, $|\varepsilon_{in}/S_{in}| < 10^{-4}$, where $S_{in} = \sum_m |\varepsilon_{inm}|$ and where ε_{inm} represents each of the m positive and negative terms contained in $\varepsilon_{in} = \sum_m \varepsilon_{inm}$. Once $\boldsymbol{q}_n$ is known one can proceed to the next position x_{n+1} along the flow and so on. We thus need to know $\boldsymbol{q}_0$ at x_0, our starting point. The stability and accuracy of the integration along x is of course crucially dependent on the magnitude of the step size Δx_n at each point x_n, and this in turn depends on the magnitude of τ_{il}.

(*b*) *Evaluation of* τ_{il}

In evaluating the coefficients τ_{il}, given by (14), some care must be exercised when catalytic species are present. To simplify the evaluation we note that

$$1/\tau_{il} = -\partial G_i/\partial q_l = -\partial F_i/\partial \xi_l,$$

since $G_i = F_i/\rho$ and $q_l = \xi_l/\rho$. Now if M catalytic bodies are involved in reaction j we must rewrite F_i in the form

$$F_i = \sum_{j=1}^{J} \psi_{ij} k_{fj} Q_j \left(\sum_{l=1}^{I} \bar{\xi}_l^{\bar{\nu}_{lj}} - \frac{1}{K_{cj}} \sum_{l=1}^{I} \xi_l^{\bar{\nu}'_{lj}} \right), \tag{15}$$

where $Q_j = \prod_{m=1}^{M} \xi_m^{\mu_{mj}}$, and we define a catalytic species to be one for which the total reactant stoichiometric coefficient $\nu_{ij} = \mu_{mj} + \bar{\nu}_{ij}$ is a nonzero integer multiple of the total product stoichiometric coefficient $\nu'_{ij} = \mu_{mj} + \bar{\nu}'_{ij}$. At least one of $\bar{\nu}_{ij}$ and $\bar{\nu}'_{ij}$ is then zero. For example, in the reaction

$$\mathrm{A} + 2\mathrm{B} \leftrightarrow \mathrm{AB} + \mathrm{B},$$

the species B is both a catalytic and a reactant species, with $\nu_B = 2$ and $\nu'_B = 1$, and hence the reaction can be rewritten as

$$A+B+M \leftrightarrow AB+M,$$

where M is the catalytic body, which happens to be the same as B, while $\bar{\nu}_B = 1$, $\mu_B = 1$ and $\bar{\nu}'_B = 0$. The importance of this distinction is to avoid converging to the trivial solution $q_B = \xi_B/\rho = 0$ when we are solving, by the present iterative method, equilibrium conditions described by $G_B = 0$, since ξ_B is a multiplicative factor of F_B and hence of G_B.

Thus, we evaluate τ_{il} from

$$1/\tau_{il} = (\partial F_i/\partial q_l)_{Q_j} + (\partial F_i/\partial q_l)_{H_j}, \tag{16}$$

where the partial derivatives are at constant Q_j and H_j respectively, and where $H_j = H_{1j} - H_{2j}$ with H_{1j} the first term within the large parentheses in (15) and H_{2j} the second. Now as equilibrium is approached the derivative at constant H_j should be set to zero in order to avoid converging to the trivial solution. A simple condition for setting $(\partial F_i/\partial q_l)_{H_j}$ to zero, at some point during the iteration, can be

$$|(H_{1j} - H_{2j})/(H_{1j} + H_{2j})| < \delta', \tag{17}$$

where $\delta' = 0{\cdot}1$ say, since at equilibrium $\delta' = 0$.

(c) *Integration Step Size*

The present iterative method allows a smooth transition from a state of chemical non-equilibrium to a state of equilibrium, and vice versa, without introducing an unnecessarily small step size as equilibrium is approached. This can be understood by first defining a characteristic length χ for changes in a species concentration q_{in-1}, due to changes in all other gas properties along the flow at x_{n-1}, by

$$|1/\chi_{in-1}| = |q_i^{-1}\, \mathrm{d}q_i/\mathrm{d}x|_{n-1}, \tag{18}$$

and also by defining a corresponding characteristic flow time $\tau'_{in-1} = \chi_{in-1}/u_{n-1}$.

Introducing finite differences we have

$$|\Delta q_{in}/q_{in-1}| \approx |\Delta x_n/\chi_{in-1}|, \tag{19}$$

and our step size can then be determined from the simple condition

$$|x_n - x_{n-1}| = \delta\,|\chi_{in-1}|, \tag{20}$$

where $0 < \delta \ll 1$. Extensive sample computations for normal shock and reservoir–nozzle flows have shown that for most cases $\delta \approx 0{\cdot}1$ should be sufficient. The thermodynamic properties of the flow and the species concentrations obtained with $\delta = 0{\cdot}05$ have been found to differ, at worst, by not more than a few per cent from those with $\delta = 0{\cdot}1$, while computations with $\delta = 0{\cdot}025$ differ from those with $\delta = 0{\cdot}05$, at worst, by less than 1%. Note that the first step size away from our

boundary condition q_0 at x_0 will need to be chosen and this is discussed later for nozzle and normal shock flows. Generally, when we are solving the gasdynamic and rate equations simultaneously we must choose χ to correspond to the gas species concentration or property (e.g. velocity, temperature, pressure) having the smallest χ value.

Condition (20) does not result in an unnecessarily small step size as equilibrium is approached. At equilibrium $\tau_{iln} \to 0$ and so the $1/\Delta t_n$ in the matrix element a_{iln} in equation (13a) becomes insignificant and we thus solve $G_i = 0$. On the other hand, when $\tau_{iln} \gg 1$ we have frozen conditions and the $1/\Delta t_n$ term dominates, so we are then solving $u\,\mathrm{d}q_i/\mathrm{d}x = 0$. Now in a state of non-equilibrium $1/\tau'_{in}$ and $1/\tau_{iln}$ are both dependent linearly on the forward rate of each reaction and so the variation of τ'_{in} (and hence χ_{in}) is coupled to the variation of τ_{iln}. However, as $\tau_{iln} \to 0$ the value of τ'_{in} becomes uncoupled from the value of τ_{iln} because τ'_{in} becomes essentially independent of the forward rate of each reaction. The value of τ'_{in} is then governed by the gradients of $q_{l\neq i}$, T, ρ and u along the flow.

(d) Convergence

The rate of convergence of the iterative method at any point x_n depends on the initial guess $\boldsymbol{q}_n^{(1)}$ for $\boldsymbol{q}_n$. A good initial guess is to set $\boldsymbol{q}_n^{(1)} = \boldsymbol{q}_{n-1}$ which will not differ appreciably from $\boldsymbol{q}_n$ since our step size in x will always be chosen such that $|(q_{in}-q_{in-1})/q_{in-1}| \ll 1$ because of conditions (19) and (20). Thus, the problem of convergence rests with the value $\boldsymbol{q}_0$ at x_0. If $\boldsymbol{q}_0$ is known then the method will always converge very rapidly, usually within five iterations, at the first step x_1, and thus at each subsequent step. When $\boldsymbol{q}_0$ is not known then it can be computed using the iterative method itself or using the free-energy minimization technique (Newman and Allison 1966). Given p_0 and T_0 we can evaluate the equilibrium concentrations $\boldsymbol{q}_0$ by solving a set of equations of the form $G_i(q_1, ..., q_I; T, \rho) = 0$ together with the atomic species conservation equations (5). Once again we need an initial guess $\boldsymbol{q}_0^{(1)}$ for $\boldsymbol{q}_0$. For a sufficiently high temperature T_0, say greater than $10T_a$, where T_a is normal room temperature, we can employ the following procedure. For those gas species which were in the initial gas mixture at T_a we take

$$q_{i0}^{(1)} = \beta_i p_0 \exp(-s)/RT_0\,, \tag{21}$$

where β_i is the fraction by volume of species i in the gas mixture and s is given by

$$s = (T/T_a)^n - 1\,, \tag{22}$$

where $0 \leqslant n < 1$. This gives the correct q_{i0} at T_a and a reasonable reduced value of $q_{i0}^{(1)}$ at high temperatures $T_0 \gtrsim 1000$ K. For example, $n = 0{\cdot}75$ gives a fair approximation for the concentration of CO_2 at $T = 5000$ K while $n = 0{\cdot}25$ does the same for O_2 and N_2 at the same temperature. For those gas species that we expect to be products of the high temperature reactions we take

$$q_{i0}^{(1)} = p_0 \exp(-D/T_0)/RT_0\,, \tag{23}$$

where D is some representative value for the activation energy of the reactions of interest. At the high temperatures extensive reservoir computations with CO_2, N_2 and air have shown that the method will converge for a wide range of initial conditions corresponding to values of n ranging between $1{\cdot}0$ and 0. For low T_0 there is another

way to obtain a reasonable first guess for $\boldsymbol{q}_0$. If the equilibrium gas concentrations $\boldsymbol{q}_*$ are known at some higher temperature T_* then we can take a small step ΔT towards T_0 and use $\boldsymbol{q}_*$ as an initial guess to obtain $\boldsymbol{q}$ at $T_*-\Delta T$. A sequence of such small temperature steps can then be repeated to obtain $\boldsymbol{q}_0$ at T_0. In order to prevent any $q_{i0}^{(r)}$ from undershooting at iteration r, we can effectively dampen the correction $\bar{q}_{i0}^{(r)}$ by the constraint that if $q_{i0}^{(r)}$ becomes negative it should be replaced by $\Omega q_{i0}^{(r-1)}$ where $\frac{1}{2} < \Omega < 1$. This constraint can also be used at any point in the flow.

Table 1. Sample computation for a reservoir containing air at $T_0 = 6500$ K and $p_0 = 1000$ atm

Tabulated are values of the concentration $\boldsymbol{q}_0$ (mol g^{-1}) for each gas constituent species at various iterations r, together with the density ρ_0 (g cm^{-3}) and mean molecular weight $\bar{M}_0$ (g mol^{-1}). Here and in Tables 2–4 E$-n \equiv$ e^{-n}

Species	$r = 1$	$r = 6$	$r = 13$	Lordi *et al.* (1966)
e^-	7·118E−9	4·774E−5	2·356E−6	2·292E−6
N_2	8·401E−3	2·424E−2	2·428E−2	2·433E−2
O_2	2·262E−3	1·345E−3	1·355E−3	1·415E−3
Ar	3·452E−4	3·448E−4	3·452E−4	3·219E−4
N	7·188E−9	4·991E−4	4·993E−4	4·881E−4
O	7·188E−9	6·987E−3	7·008E−4	6·888E−3
NO	7·188E−9	4·757E−3	4·778E−3	4·768E−3
NO^+	7·188E−9	4·774E−5	2·356E−6	2·292E−6
ρ_0	5·432E−2	4·894E−2	4·899E−2	4·906E−2
$\bar{M}_0$	2·897E+1	2·610E+1	2·613E+1	2·617E+1

As an example, let us consider a reservoir containing air (78% N_2, 21% O_2 and 1% Ar) at $T_0 = 6500$ K and $p_0 = 1000$ atm (1 atm $\equiv$ 101 325 Pa) (cf. Lordi *et al.* 1966) and we wish to evaluate $\boldsymbol{q}_0$, ρ_0 and $\bar{M}_0$, where $\bar{M}_0$ is the mean molecular weight. To do this D is set equal to 10^5 K, with $n = 0{\cdot}25$ and $\Omega = 0{\cdot}75$, while $\beta_{N_2} = 0{\cdot}78$, $\beta_{O_2} = 0{\cdot}21$ and $\beta_{Ar} = 0{\cdot}01$. Table 1 gives $\boldsymbol{q}_0^{(r)}$, ρ_0 and $\bar{M}_0$ at various iteration steps r. The final values are in excellent agreement with the results of Lordi *et al.* who performed the same computation but with $\beta_{Ar} = 0{\cdot}0093$. Most species have converged almost to two decimal places by the sixth iteration, however the charged species take longer. This is due to the fact that charge balance has been ensured at each iteration by computing the electron concentration q_{k0} directly from (5); thus

$$q_{k0} = C_k - \sum_{i \neq k}^{I} \alpha_{ki} q_{i0}, \tag{24}$$

where $C_k = 0$ and all the α_{ki} are negative. This approach can be applied also to non-equilibrium cases. However, the form of the modified Jacobian matrix **A** should always be the same as (13), and the corrections $\bar{q}_{k0}$ for the electrons are simply ignored.

3. Gasdynamic Equations for Nozzle and Normal Shock Flows

In order to obtain the chemical composition and thermodynamic state of a gas in quasi-one-dimensional steady adiabatic inviscid flows within nozzle systems or behind normal shocks we must solve the coupled gasdynamic equations consistently

with the system of coupled concentration rate equations. If p denotes the gas pressure, ρ the density and u the velocity then we may write the conservation of mass, momentum and energy equations respectively as

$$\rho u A(x) = \text{const.}, \tag{25}$$

$$\rho u \frac{du}{dx} + \frac{dp}{dx} = 0, \tag{26}$$

$$h + \tfrac{1}{2}u^2 = \text{const.} \tag{27}$$

Here $A(x)$ is the cross sectional area confining the flow and h is the gas enthalpy given by

$$h = \sum_{i=1}^{I} h_i q_i M_i, \tag{28a}$$

where q_i represents the concentration of gas species i in mol g^{-1} and M_i is the molecular weight in g mol^{-1}, while h_i is the enthalpy in erg g^{-1} (1 erg = 10^{-7} J). The specification of h_i requires a molecular model (see e.g. Stull and Prophet 1971). Here we take h_i to be

$$h_i(T) = h_{fi} + R_i T \left(\sum_n \frac{g_n(\theta_n/T)}{\exp(\theta_n/T) - 1} + n_r + \tfrac{3}{2} + 1 \right.$$
$$\left. + \sum_l g_l \varepsilon_l \exp(-\varepsilon_l/T) \Big/ \sum_l g_l \exp(-\varepsilon_l/T) \right), \tag{28b}$$

where h_{fi} is the heat of formation and R_i the gas constant of species i. The first term within the large parentheses corresponds to the energy of vibration, assuming vibrational equilibrium, summed over all possible modes of vibration. The second term corresponds to the rotational energy with $n_r = 1$ for linear and $\frac{3}{2}$ for nonlinear molecules. The third term corresponds to the translational energy, the fourth is due to the energy associated with the partial pressure of the gas species and the last term corresponds to the energy due to electronic levels of energy ε_l and statistical weight g_l. To these gasdynamic equations we add the $I-K$ rate equations of the form (4) and K atomic conservation equations of the form (5). To complete the system of equations we add the state equation

$$p = \rho R T / \bar{M}, \tag{29}$$

where R is the universal gas constant and $\bar{M}$ is the mean molecular weight of the gas given by

$$\bar{M} = \sum_i q_i M_i \Big/ \sum_i q_i. \tag{30}$$

Thus, equations (4) and (5) and (25)–(29) constitute $I+4$ equations in the $I+4$ unknowns p, ρ, u, T and q_i for $i = 1, 2, \ldots, I$. Before we can solve such a system of equations we first need to know the expected behaviour of the velocity field $u(x)$.

(a) Subsonic–Supersonic Flow

If the gas flow goes from subsonic to supersonic, as can be the case in Laval nozzle flows initiated by a high enthalpy reservoir, then we may solve for the velocity by combining (25), (26) and (29) to obtain

$$\frac{1}{u}\frac{\mathrm{d}u}{\mathrm{d}x} = \left(\frac{1}{A}\frac{\mathrm{d}A}{\mathrm{d}x} + \frac{1}{\overline{M}}\frac{\mathrm{d}\overline{M}}{\mathrm{d}x} - \frac{1}{T}\frac{\mathrm{d}T}{\mathrm{d}x}\right) \Big/ \left(\frac{u^2}{v^2} - 1\right) = \frac{f(A, \overline{M}, T)}{g(u, v)}, \tag{31}$$

where $v^2 = RT/\overline{M}$, the isothermal speed of sound. We see that if $u < v$ then $g(u, v) < 0$ and so $f(A, \overline{M}, T) < 0$, if $\mathrm{d}u/\mathrm{d}x$ is to be positive. Similarly if $u > v$ then $g(u, v) > 0$ and $f(A, \overline{M}, T)$ must be positive. Now if $\mathrm{d}u/\mathrm{d}x$ is to remain finite when $u = v$ then

$$f(A, \overline{M}, T)_{u=v} = 0. \tag{32}$$

This gives us a boundary condition on u since A, $\overline{M}$ and T are functions of x and so $f(x) = 0$ when $u = v$ at some point $x = x_c$. We can then integrate (31) upstream or downstream from x_c to obtain $u(x)$. To do this we first need to obtain $u^{-1}\,\mathrm{d}u/\mathrm{d}x$ at $x = x_c$ and this can be done by using L'Hopital's theorem, which results in the quadratic equation

$$a(\mathrm{d}u/\mathrm{d}x)_c^2 + b(\mathrm{d}u/\mathrm{d}x)_c + c = 0, \tag{33}$$

at $x = x_c$. The coefficients a, b and c are given by

$$a = \frac{2}{v^2}, \qquad b = -\frac{2}{v}\frac{\mathrm{d}v}{\mathrm{d}x}, \qquad c = -\frac{1}{A}\frac{\mathrm{d}^2A}{\mathrm{d}x^2}.$$

One can then use the Euler-trapezoidal rule to integrate (31). In order to obtain x_c and thus u_c and $(\mathrm{d}u/\mathrm{d}x)_c$ we need to solve (32) and to do this we need to know $A(x)$, $\overline{M}(x)$ and $T(x)$ for all x. However, since we expect the isothermal sonic point x_c to lie upstream of the throat of the nozzle, we need only know $A(x)$, $\overline{M}(x)$ and $T(x)$ for the region between the reservoir and the nozzle throat before we can solve for $u(x)$ in that region. We can then obtain the density $\rho(x)$ from the continuity equation (25) and the pressure $p(x)$ from the state equation (29).

(b) Subsonic Flow or Supersonic Flow

If the flow remains subsonic as is the case behind a normal shock, or supersonic as is the case beyond the throat of a nozzle, we can use the trapezoidal rule to integrate (26) directly, given u_0 and p_0 at some point x_0. This results in the following expression for $p(x)$ at $x = x_0 + \Delta x$, where Δx is small:

$$p(x) = \alpha\beta_0 p_0 + \alpha\rho_0 u_0^2(1 - \alpha\rho_0/\rho)/\beta, \tag{34}$$

where

$$\alpha = A(x_0)/A(x), \qquad \beta = 1 - \Delta x\, A'(x)/2A(x), \qquad \beta_0 = 1 + \Delta x\, A'(x_0)/2A(x_0),$$

with $A'(x) = \mathrm{d}A/\mathrm{d}x$. Note that if $A(x)$ is constant then $\alpha = 1$ and $\beta = \beta_0 = 1$, and (34) reduces to the standard simple form

$$p(x) = p_0 + \rho_0 u_0^2(1 - \rho_0/\rho). \tag{35}$$

We can then obtain the density from the state equation:

$$\rho(x) = p(x)\,\overline{M}(x)/RT(x), \tag{36}$$

and the velocity from continuity:

$$u(x) = \dot{M}/\rho(x)\,A(x), \tag{37}$$

where the mass flow $\dot{M} = \rho_0 u_0 A_0$ is constant. Thus, in this case we need to know $A(x)$, $\overline{M}(x)$ and $T(x)$ only at the point x in order to obtain $u(x)$.

(c) Method of Solution

It is evident from the preceding in this section that we need two different methods in order to solve for p, ρ, u, T and the q_i. In the case of subsonic–supersonic flow within a nozzle we initially set $\mathrm{d}\overline{M}/\mathrm{d}x = 0$ and $T(x) = T_0$ in the region $x_0 < x \leqslant x_*$, where x_0 and x_* are the locations of the reservoir and throat respectively, and thus obtain $u(x)$ from (31), $\rho(x)$ from (25) and a new $T(x)$ from (27). We can then obtain the $q_i(x)$ and $\overline{M}(x)$. The process is then repeated until $u(x)$, $\rho(x)$, $T(x)$, $\overline{M}(x)$ and the $q_i(x)$ are known for points up to the throat. Beyond the throat we can solve iteratively at each point equations (27), (34), (36) and (37) for $T(x)$, $p(x)$, $\rho(x)$ and $u(x)$ respectively, together with the rate equations (4) and (5) to obtain all the $q_i(x)$. In practice one needs to go a little distance downstream of the throat using the former method since any small errors in $T(x)$ can result in $f(A, \overline{M}, T)$ and $g(u, v)$ having the wrong sign, resulting in a negative velocity gradient.

Now in order to solve (27) for $T(x)$ we assume that $u(x)$ is given and we rearrange the equation into the form

$$h(T) + \tfrac{1}{2}u^2 - c_0 = 0, \tag{38}$$

where $c_0 = h(T_0) + \frac{1}{2}u_0^2$ is the total energy at $x = x_0$. We may now employ the standard Newton–Raphson technique to iteratively solve (38) for T.

Thus, in total we have three iterative loops. One solves for the $q_i(x)$ given $T(x)$ and $\rho(x)$ using the iterative method of Section 2*a*. Another solves iteratively the energy equation (38) for $T(x)$ by taking $u(x)$ as being given, but evaluating the $q_i(x)$ at each temperature iteration. The third loop solves the gasdynamic equations for $u(x)$, $\rho(x)$, $p(x)$ and $\overline{M}(x)$ given $T(x)$ and the $q_i(x)$. All three iterative loops usually converge within five iterations for each.

A fourth iterative loop may be necessary if one includes the depression of the ionization potential due to Coulomb interactions if the gas is ionized. This fourth iterative loop is due to the fact that the extent to which the ionization potential is decreased depends on the $q(x)$ of the ionized species and this depends on $K_c(T)$, the equilibrium reaction constant for an ionization reaction, which in turn depends on the depression of the ionization potential. We now examine the form of $K_c(T)$ in the presence of Coulomb interactions.

(d) Coulomb Interactions

The equilibrium reaction constant may be written in the form

$$K_c(T) = \prod_i \left(\frac{Q_i}{N_A V}\right)^{\psi_i} \exp(-D/T), \tag{39}$$

with $Q_i = Q_{tr} Q_{vb} Q_{rt} Q_e$, where each Q represents the partition function for each mode of energy storage of species i. In the present model

$$Q_e = \sum_l g_l \exp(-\varepsilon_l/T), \quad Q_{vb} = \prod_n \frac{1}{1-\exp(-\theta_n/T)},$$

$$Q_{tr} = V(2\pi mkT/h^2)^{3/2}, \quad Q_{rt} = T^{n_r}/\sigma^{\theta_r},$$

where k is Boltzmann's constant, h is Planck's constant, m is the molecular mass, σ is a symmetry factor that is 2 for homonuclear and 1 for heteronuclear molecules and θ_r is the characteristic temperature for rotation. The volume of gas is represented by V and N_A is Avogadro's number. Since Q_{tr} linearly depends on V we see that K_c is independent of V. The parameter D is the activation temperature for the reaction and is given by

$$D = \frac{1}{R} \sum_{i=1}^{I} \psi_i M_i h_{fi}, \tag{40}$$

where the summation is over all the species taking part in the reaction. In the presence of Coulomb interactions the ionization potential D of the ions is reduced as well as the total gas pressure and enthalpy.

It can be shown (see Zeldovich and Raizer 1966) that due to Coulomb interactions the total internal energy of the gas is reduced by an amount

$$E_C = -e^3 \left(\frac{\pi}{kT}\right)^{\frac{1}{2}} \left(\sum_{i=1}^{I} n_i Z_i^2\right)^{3/2}, \tag{41}$$

where e is the electronic charge, $n_i = \rho N_A q_i$ is the number density and $Z_i e$ is the electronic charge of species i. If e is in $(\text{erg cm})^{\frac{1}{2}}$ and n_i in cm^{-3} then E_C is in erg cm^{-3}. Because of the reduction in the internal energy, the chemical potential of each species carrying a charge is reduced and so is D by an amount

$$D_C = E_C \sum_{i=1}^{I} \psi_i Z_i^2 \Big/ k \sum_{i=1}^{I} n_i Z_i^2. \tag{42}$$

Similarly, the pressure and enthalpy are reduced by

$$P_C = \tfrac{1}{3} E_C, \qquad h_C = 4p_C/\rho,$$

where h_C is in erg g^{-1}. The correction p_C alters the velocity equation (31) by changing v^2 to

$$v^2 = wRT/\overline{M}, \tag{43}$$

where $w = 1 + \frac{3}{2} p_C/p$. The corrections p_C and h_C are usually small and can be neglected but D_C can be significant. It should be noted that the above Coulomb corrections are based on the Debye–Hückel method which is valid only when the Debye radius $d \gg r_0$, the mean distance between the charged particles. This condition essentially reduces to the condition that D_C is small compared with T (Zeldovich and Raizer 1966).

4. Sample Computations

(a) *Reservoir–Nozzle Flows*

For steady real gas flows within a converging–diverging nozzle, initiated by a high enthalpy reservoir, the reservoir values of the species concentrations q_0 together with ρ_0 and $\overline{M}_0$ can be obtained by employing the techniques described in Section 2 given T_0, p_0 and the gas mixture. The first computation is a nozzle flow initiated by a reservoir containing air at $p_0 = 100$ atm and $T_0 = 8000$ K. The nozzle cross sectional area is taken to be axisymmetric and varies with the distance x', measured from the throat, according to the hyperbolic law $A/A_* = 1+(x'/l)^2$, where $A_* = 1\,\text{cm}^2$ and $l = R_*/\tan\theta = 1$, and where R_* is the throat radius while θ is the semi-angle of

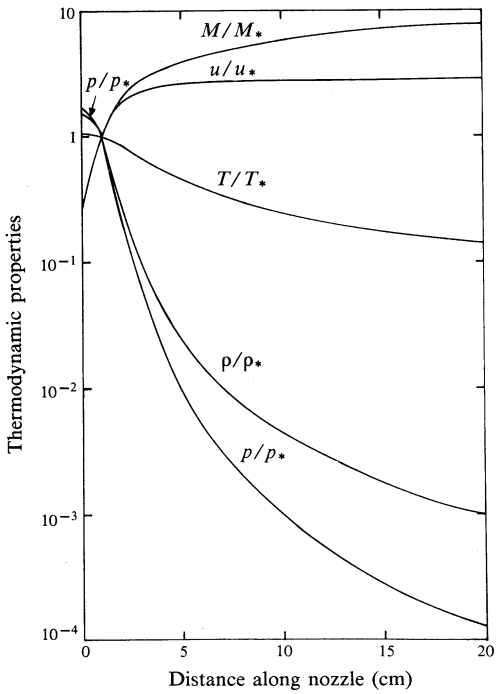

Fig. 1. Variation of gas pressure p, density ρ, temperature T, velocity u and frozen Mach number M_f as functions of the distance along a nozzle for a flow initiated by a reservoir containing air at $p_0 = 100$ atm and $T_0 = 8000$ K. The throat values are $p_* = 59{\cdot}87$ atm, $\rho_* = 2{\cdot}164\times10^{-3}\,\text{g cm}^{-3}$, $T_* = 7514$ K, $u_* = 1{\cdot}817\times10^5\,\text{cm s}^{-1}$ and $M_* = 0{\cdot}9314$.

the asymptote cone. The reservoir is taken to be 1 cm upstream from the throat. The above conditions together with the reactions and reaction rates are taken from Eschenroeder *et al.* (1962) for reasons of comparison. The variation of T, p, ρ, u and frozen Mach number M_f along the nozzle is given in Fig. 1 and we note especially the variation of u and T upstream of the throat. In this region the deviation of T from T_0 is a few per cent while u increases substantially. It is this almost isothermal behaviour of the flow upstream of the throat that produces the very fast convergence of the subsonic velocity field, when the iterative method described in Section 3*c* is used, since the main unknown in equation (31) is the temperature structure in this region. Thus, setting $T = T_0$ for all $x' < 0$ results in a very good first approximation for the subsonic u. Note that the frozen sonic point $M = 1$ singularity occurs just beyond the throat while the isothermal sonic point (32) lies upstream of the throat. In addition, since in the iterative method we first solve for u before q, by integrating the velocity equation (31) from the isothermal sonic point x_c to the reservoir $x = 0$,

the first step away from x_c can be computed using u_c and (du/dx_c). Now since u undergoes the largest variation, amongst all the gas properties upstream of the throat, its characteristic relaxation length (18) determines the x grid in that region. Beyond the throat it is the variation of the chemical species concentrations that determines the step size. This variation is shown in Fig. 2 together with the results of Eschenroeder *et al.* (1962). It can be seen that there is excellent agreement between the two sets of results.

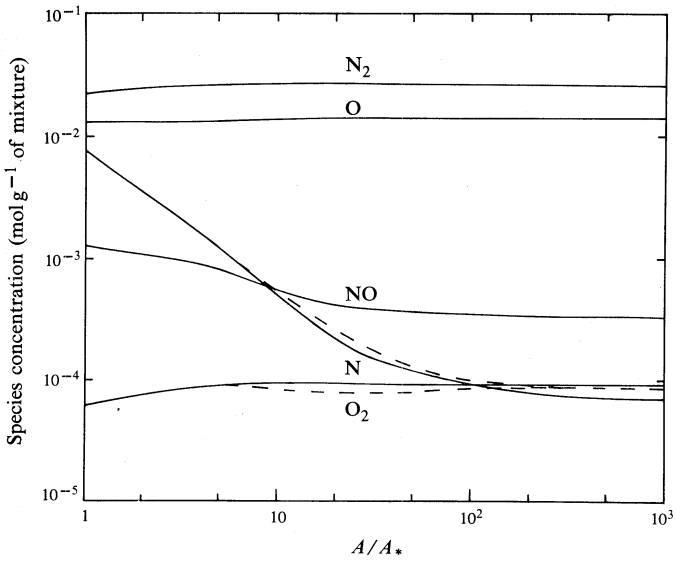

Fig. 2. Species concentrations as functions of the cross sectional area ratio A/A_* for the case described in Fig. 1. The solid curves are for the present work and the dashed curves are from Eschenroeder *et al.* (1962).

As a further comparison example, the species concentrations are computed for a nozzle flow initiated by a reservoir containing CO_2 at $T_0 = 10\,000$ K and $p_0 = 200$ atm. The nozzle is taken to be a cone with semi-angle $7{\cdot}5°$ whose cross sectional area varies according to $A/A_* = 1 + 2x'/l + (x'/l)^2$, where $l = 4{\cdot}75$ and $R_* = 0{\cdot}625$ cm. The same computation was performed by Ebrahim and Hornung (1973) and Ebrahim (1975) from where the reactions and reaction rates are taken. As can be seen in Fig. 3 there is substantial disagreement between their results and the present calculations, especially for CO_2 and O_2. Their results were obtained using the method of Lordi *et al.* (1966) and the only difference between their molecular model (a simple harmonic oscillator) and the present is that they have assumed a mean characteristic vibrational temperature $T_\theta = 1807$ K for all the four vibrational modes of CO_2 (Ebrahim 1975), whereas in the present work vibrational modes are assigned their true vibrational temperatures, i.e. $T_{\theta 1,2} = 960{\cdot}9$ K for the bending mode (degeneracy 2), $T_{\theta 3} = 1933{\cdot}7$ K for the symmetric and $T_{\theta 4} = 3383$ K for the asymmetric stretch modes. The use of $T_\theta = 1807$ K was considered by Ebrahim as being a reasonable approximation for gas temperatures of the order of T_θ or higher. However, as can be seen in Table 2 the above assumption produces errors greater than 100% for the equilibrium concentration of CO_2 even at temperatures well in excess of T_θ. It should be noted that

for equilibrium CO_2 at $T_0 = 10000$ K and $p_0 = 200$ atm one should also include the species C_2, O_2^+, O^-, O_2^- and C^- as shown by the computations of Miller and Wilder (1976); however, for comparison reasons we have not included these here. The differences in the CO_2 concentrations along the nozzle cannot be solely explained by the use of $T_\theta = 1807$ K since the strong inflection point found by Ebrahim and

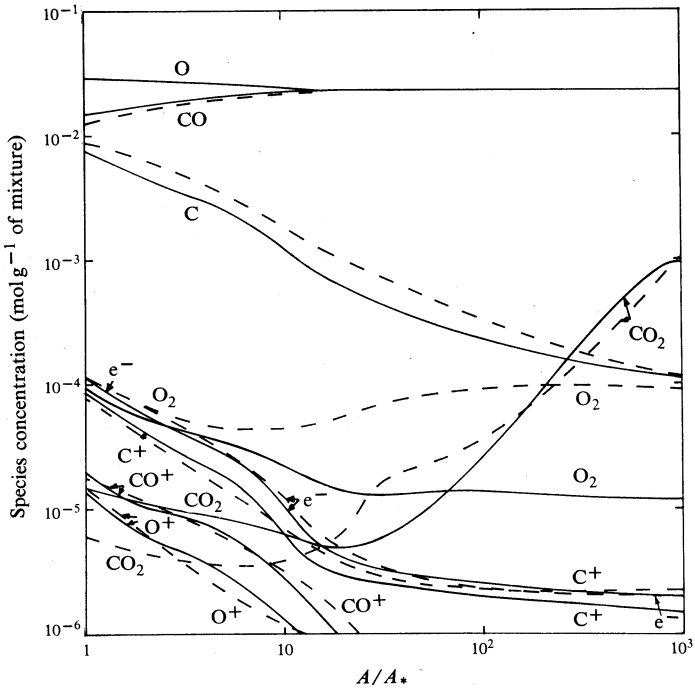

Fig. 3. Species concentrations along a nozzle for a gas flow initiated by a high enthalpy reservoir containing CO_2 at $p_0 = 200$ atm and $T_0 = 10000$ K. The solid curves are for the present work and the dashed curves are from Ebrahim and Hornung (1973).

Table 2. Equilibrium species concentrations (mol g^{-1} of mixture) for CO_2 at $T = 5700$ K and $p = 200$ atm

The results of Miller and Wilder (1976) are compared with those obtained by the present iterative method using four vibrational modes for CO_2 (case A) and one mean vibrational mode (case B)

Species	Miller & Wilder	A	B
CO_2	4·081E−2	4·298E−2	2·528E−2
CO	5·289E−1	5·254E−1	5·358E−1
C	2·212E−5	2·238E−5	2·250E−5
O_2	9·873E−2	9·385E−2	9·654E−2
O	3·315E−1	3·378E−1	3·427E−1

Hornung near $A/A_* = 30$ does not occur in the present work even when $T_\theta = 1807$ K is used. It appears then that this inflection point is a computational artifact. This was borne out by another computation for a gas flow within the same nozzle but initiated by a reservoir containing CO_2 at $T_0 = 20000$ K and $p_0 = 400$ atm. It is rather

difficult to reconcile such very strong local variations in the concentration of CO_2 with the rather smooth variation of all the other species.

Table 3. Equilibrium species concentrations (mol g^{-1} of mixture) for two CO_2 reservoir conditions with the effects of Coulomb interactions included (C) and excluded (NC)

Species	$T = 10000$ K and $p = 200$ atm		$T = 20000$ K and $p = 400$ atm	
	C	NC	C	NC
C	0·930E−2	0·930E−2	0·132E−1	0·153E−1
O	0·319E−1	0·319E−1	0·384E−1	0·404E−1
CO_2	0·168E−4	0·169E−4	0·218E−8	0·311E−8
CO	0·132E−1	0·133E−1	0·301E−4	0·388E−4
O_2	0·124E−3	0·124E−3	0·796E−5	0·930E−5
e^-	0·192E−3	0·170E−3	0·165E−1	0·122E−1
C^+	0·138E−3	0·122E−3	0·945E−2	0·732E−2
O^+	0·237E−4	0·209E−4	0·702E−2	0·494E−2
CO^+	0·302E−4	0·267E−4	0·182E−4	0·156E−4

In Table 3 the changes in the equilibrium species concentrations are given, for two reservoir conditions, when the depression of the ionization potential due to Coulomb interactions is included. It can be seen that the effects of the Coulomb interactions become more pronounced as the electron concentration is increased. For the lower temperature conditions the average correction to the ionization potential is $D_C/D \approx -0{\cdot}02$ with $|D_C/T| \approx 0{\cdot}24$, while at the high temperature $D_C/D \approx -0{\cdot}10$ and $|D_C/T| \approx 0{\cdot}65$. Since the evaluation of D_C is based on the Debye–Hückel method, whose applicability is valid for values of $|D_C/T| < 1$, we see that at $T = 20000$ K and $p = 400$ atm we are close to this limit for CO_2. This is in keeping with the results of Zeldovich and Raizer (1966, p. 218) where they gave $D_C/D \approx -0{\cdot}10$ and $|D_C/T| \approx 0{\cdot}63$ for air at $T = 100000$ K and $p = 727{\cdot}6$ atm.

(b) Reflected-type Shock-tube–Nozzle Flow

For a reflected-type shock tube we must obtain the equilibrium conditions behind the initial shock, behind the reflected shock and in the stagnation region (Stalker 1967) in order to obtain the reservoir conditions which initiate the nozzle flow. Given the initial pressure p_0, temperature T_0 and initial shock velocity u_0 we can apply the method of Section 3*b* together with (34) and the iterative method described in Section 3*c* to obtain the equilibrium conditions T_1, p_1, ρ_1, q_1 and u_1 (in the shock frame SF) behind the initial shock, and so obtain $u_g = u_0 - u_1$, the velocity of the gas in the laboratory frame (LF). Knowing u_g we can then obtain the equilibrium conditions behind the reflected shock by evaluating $u_2 = u_g(1 - \rho_1/\rho_3)$ in front of the reflected shock, with ρ_3 being the density behind the reflected shock. Finally, when the gas behind the reflected shock is brought to rest by the contact surface we obtain the stagnation conditions by setting $u_s = 0$ (LF). The stagnation pressure p_s is obtained experimentally and T_s is obtained by assuming that the gas undergoes an isentropic expansion or compression from p_3 to p_s (Stalker 1967). In this case we solve

$$T\,s(T) = \sum_{i=1}^{I} (h_i - \mu_i) q_i M_i = \text{const}. \tag{44}$$

to obtain T_s, where $s(T)$ is the total entropy in erg g^{-1} K^{-1} and μ_i is the chemical potential of species i given by

$$\mu_i(T) = -R_i T ln(Q_i/N_i) + h_{fi}, \tag{45}$$

and where $N_i = n_i V$ and Q_i is the total partition function of species i. We note that any Coulomb modifications to μ_i and h_i are identical so they cancel.

Table 4. Sample computations for N_2 within a reflected-type shock-tube–nozzle system

Concentration q (mol g^{-1}), T, p and mean molecular weight $\overline{M}$ are given for each gas species for the initial shock-tube conditions, behind the initial shock, behind the reflected shock, within the stagnation region and at the nozzle exit. The frozen Mach number M_f is given in front of the initial and reflected shocks (in the SF) together with the Mach number of the flow (in the LF) at the nozzle exit

Species	Initial conditions	Initial shock	Reflected shock	Stagnation conditions	Nozzle exit conditions
e^-		1·4386E−6	3·8352E−5	2·5733E−5	4·9919E−7
N_2	3·5696E−2	3·2917E−2	2·4944E−2	2·6098E−2	3·1348E−2
N		5·5586E−3	2·1453E−2	1·9156E−2	8·6961E−3
N^+		6·0952E−7	2·4643E−5	1·6365E−5	4·9897E−7
N_2^+		8·2907E−7	1·3709E−5	9·3675E−6	2·2070E−10
T	2·9600E+2	6·8845E+3	9·6569E+3	9·0655E+3	1·3393E+3
p	1·3546E+5	3·1385E+7	3·3715E+8	1·8296E+8	1·1050E+4
$\overline{M}$	2·8014E+1	2·5989E+1	2·1520E+1	2·2070E+1	2·4972E+1
M_f		1·3594E+1	2·9819E+0		7·2883E+0

Table 5. Reactions and constants used for evaluation of the forward rate $k_f = CT^n \times \exp(-\varepsilon/T)$ for N_2 flow in a shock-tube–nozzle system with stagnation conditions $T_s = 9066$ K and $p_s = 1{\cdot}83 \times 10^8$ dyne cm^{-2}

Numbers in parentheses for C represent powers of 10

Reaction	Catalyst M	C	n	ε (K)
$N_2 + M \rightarrow 2N + M$	N_2	3·70(21)	−1·6	113 227
$N_2 + M \rightarrow 2N + M$	N	1·60(22)	−1·6	113 227
$N_2^+ + e^- \rightarrow 2N$		1·00(22)	−1·5	0
$N^+ + e^- + M \rightarrow N + M$	N	6·00(24)	−2·5	0
$N^+ + e^- + M \rightarrow N + M$	N_2	2·22(26)	−2·5	0
$N_2^+ + N \rightarrow N + N^+$		7·80(11)	0·5	0
$N_2^+ + e^- + M \rightarrow N + M$	N	6·00(24)	−2·5	0
$N_2^+ + e^- + M \rightarrow N + M$	N_2	2·00(26)	−2·5	0
$N^+ + e^- + M \rightarrow N + M$	e^-	1·70(38)	−4·5	0
$N_2^+ + e^- + M \rightarrow N + M$	e^-	1·70(38)	−4·5	0

Table 4 presents the species concentrations and the thermodynamic conditions at the various stages which set up the shock-tube stagnation conditions and at the nozzle exit for N_2 flow. The reactions and the relevant constants for evaluating the forward rate $k_f = CT^n \exp(-\varepsilon/T)$ for each reaction are given in Table 5, while the equilibrium constants K_c can be evaluated using (39). The throat cross sectional area of the nozzle is $A_* = 1$ cm^2 and the area varies with the distance x', measured in cm from the throat, as

$$A/A_* = 1 - a_1 x' + a_2 x'^2, \qquad -5 \leqslant x' \leqslant 0$$
$$= 1 + a_1 x' + a_2 x'^2, \qquad 0 \leqslant x' \leqslant 25{\cdot}4$$

$$= b_1 + b_2 x' + b_3 x'^2 - b_4 x'^3 + b_5 x'^4 - b_6 x'^5 + b_7 x'^6, \qquad 25{\cdot}4 \leqslant x' \leqslant 138,,$$

where

$$a_1 = 0{\cdot}555, \quad a_2 = 0{\cdot}071, \quad b_1 = 0{\cdot}043, \quad b_2 = 0{\cdot}150, \quad b_3 = 0{\cdot}131,$$

$$b_4 = 1{\cdot}53 \times 10^{-3}, \quad b_5 = 7{\cdot}47 \times 10^{-6}, \quad b_6 = 1{\cdot}76 \times 10^{-8}, \quad b_7 = 1{\cdot}76 \times 10^{-11}.$$

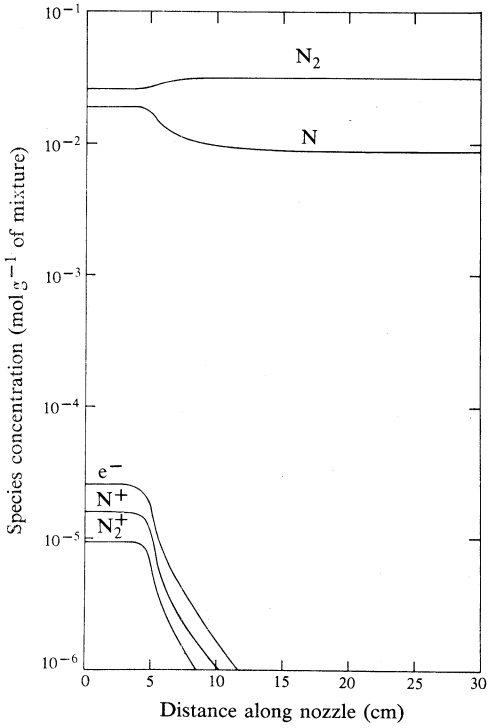

Fig. 4. Species concentrations along a nozzle for a gas flow initiated by the stagnation region of a reflected-type shock tube containing N_2. The stagnation conditions are $p_s = 1{\cdot}83 \times 10^8$ dyne cm^{-2} ($\equiv 1{\cdot}83 \times 10^7$ Pa) and $T_s = 9066$ K.

Thus the nozzle cross sectional area has a continuous first derivative at the throat. A plot of the species concentrations along the nozzle is given in Fig. 4, where the distance is measured in cm from the nozzle entrance and the throat is located at $x = 5$ cm.

(*c*) *Flows behind Normal Shocks*

In order to obtain both the chemical and flow properties of the gas behind a normal shock we can employ the concepts described in Section 2 to obtain the equilibrium species concentrations q_a, density ρ_a and mean molecular weight $\bar{M}_a$ in front of a normal shock given p_a, T_a and u_a. Assuming that the species concentrations q_b across the shock remain frozen to the equilibrium values in front of the shock (Vincenti and Kruger 1977), i.e. $q_b = q_a$ for $u_a > a_f$, where a_f is the frozen sound speed, we can use the shock jump conditions given in Section 3*b* to obtain T_b, p_b, ρ_b and u_b in the SF. As noted in Section 2*c*, the first step size in the numerical integration of the equations must be chosen. In the case of flows behind normal shocks this choice crucially depends on the shock relaxation length x_r, the distance behind the

shock where chemical equilibrium is reached. The first step Δx_0 should be less than the local characteristic relaxation length of each gas property undergoing changes along the flow and it must also satisfy $\Delta x_0 \ll x_r$. Since x_r can vary by orders of

Table 6. Variation of chemical relaxation length x_r behind a normal shock in N_2 with frozen Mach number M_{fa} and pressure p_a in front of the shock

p_a (dyne cm^{-2})	$M_{fa} = 11{\cdot}40$	x_r (cm) $= 14{\cdot}26$	$= 19{\cdot}96$
10^4	16·90	1·300	0·150
10^5	1·600	0·050	0·005

Table 7. Frozen Mach number M_{fa} in front of the shock, relaxation length x_r, temperature ratio T_b/T_a across the shock and equilibrium temperature T_E for nitrogen, air and carbon dioxide

Conditions in front of the shock are $p_a = 10^4$ dyne cm^{-2}, $T_a = 296$ K and $u_a = 5 \times 10^5$ cm s^{-1}

Thermodynamic properties	N_2	Gas Air	CO_2
M_{fa}	14·26	14·50	18·62
x_r (cm)	1·30	0·10	0·09
T_b/T_a	32·87	33·56	31·70
T_E/T_a	21·48	19·75	14·12

magnitude depending on the initial conditions in front of the shock, some knowledge is needed of the expected magnitude of x_r. To this end, through trial and error, two tables have been constructed which give x_r as a function of p_a, M_{fa} (frozen Mach number in front of the shock) and type of gas. In view of the fact that the present method is an iterative one, a very small first step cannot be chosen as the method will converge extremely slowly for those species which may be in chemical equilibrium immediately behind the shock, as can be seen by the form of a_{iln} in equation (13). Table 6 gives the chemical relaxation length x_r behind a normal shock in N_2 as a function of M_{fa} and p_a. The value of x_r is determined at the point behind the shock where $T/T_E \approx 1{\cdot}05$, with T_E the temperature when equilibrium is reached. We see that as M_{fa} increases x_r decreases, while for a fixed M_{fa} the width decreases with increasing p_a. Table 7 gives a comparison of M_{fa}, x_r, T_b/T_a and T_E/T_a for N_2, air and CO_2 for a normal shock with conditions $p_a = 10^4$ dyne cm^{-2}, $T_a = 296$ K and $u_a = 5 \times 10^5$ cm s^{-1}. The temperature jump T_b/T_a across the shock does not vary greatly between the gases although T_E does. The relaxation zone is shorter in air and CO_2 relative to that in N_2 due to the lower dissociation temperature of O_2 and CO_2. Fig. 5 demonstrates the effect of a variable cross sectional area confining the flow behind a normal shock in N_2 with $p_a = 10^4$ dyne cm^{-2}, $T_a = 296$ K, $u_a = 7 \times 10^5$ cm s^{-1} and $M_{fa} = 19{\cdot}96$. The area is given by $A = a + bx$, where $a = 1$ cm^2 and $b = 0$, 100, 1000 cm. We see that as b increases x_r decreases: for $b = 0$, 100 and 1000 cm the relaxation length x_r takes the values 0·15, 0·04 and 0·014 cm respectively. Thus, with the help of Tables 6 and 7 and Fig. 5 one can obtain a rough estimate of x_r and so choose $\Delta x_0 = x_r/100$ say.

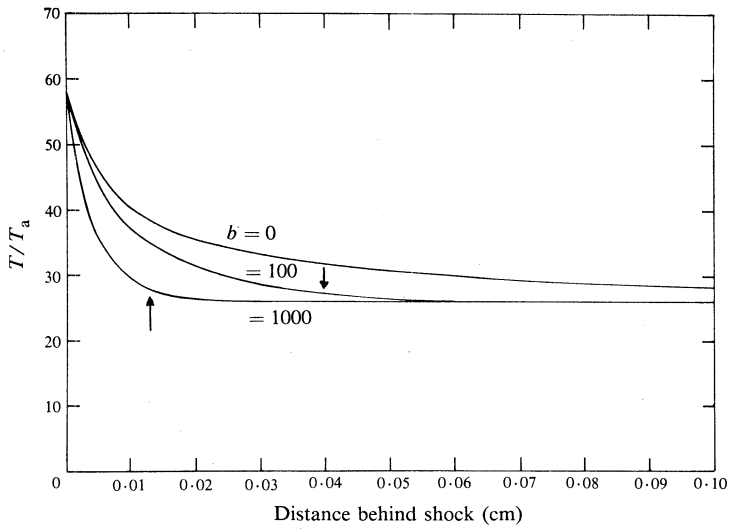

Fig. 5. Variation of gas temperature behind a normal shock with $p_a = 10^4$ dyne cm^{-2}, $T_a = 296$ K, $u_a = 7 \times 10^5$ cm s^{-1} and $M_{fa} = 19{\cdot}96$ in front of the shock. A variable cross sectional area $A = 1 + bx$ (cm^2) confines the flow behind the shock. The arrows point to the location where chemical equilibrium is achieved.

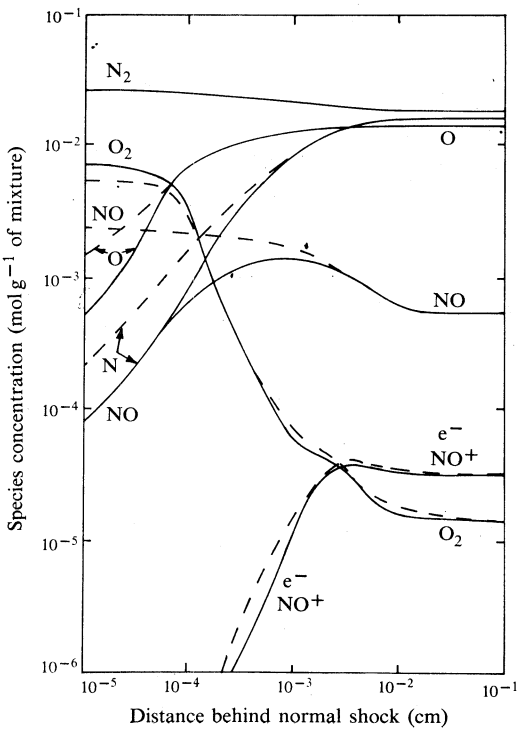

Fig. 6. Species concentrations behind a normal shock in air with $p_a = 1$ in. Hg, $T_a = 296$ K and $u_a = 6{\cdot}579 \times 10^5$ cm s^{-1} in front of the shock. The solid curves are for the present work and the dashed curves from McIntosh (1971).

Fig. 6 gives the variation of the species concentrations behind a normal shock in air for $T_a = 296$ K, $p_a = 1$ in. Hg ($\equiv 3386{\cdot}4$ Pa) and $u_a = 6{\cdot}579 \times 10^5$ cm s^{-1}. These conditions are chosen to be the same as those used by McIntosh (1971) who computed the variation of the species concentrations using the method of Garr *et al.* (1966). Although their computer code fails to make a smooth transition from non-equilibrium into the equilibrium state of the gas, the concentrations given by McIntosh have been extrapolated to their equilibrium values. There is generally a good agreement between the two sets of results; however, the variation of the NO concentration close to the shock given by McIntosh seems unrealistic as it monotonically increases towards the shock. The NO concentration computed in our work is first quite small, since it is assumed that the concentration is frozen across the shock, then increases as N_2 and O_2 dissociate, and finally decreases as it undergoes dissociation itself.

5. Conclusions

An iterative method has been presented that allows the full thermochemical state of the gas to be modelled for steady adiabatic inviscid flows within nozzles and behind normal shocks. The method's iterative nature allows the velocity field within nozzles to be easily computed and the effects of Coulomb interactions to be incorporated into the model. Further, a simple condition has been given for evaluating the integration step size which ensures both stability and accuracy in the integration of the coupled rate equations and gasdynamic equations. Generally, not more than 50 integration steps along the flow are required for both nozzle and normal shock flows. In the case of flows behind a normal shock, criteria have been discussed for determining a rough estimate of the relaxation length behind the shock and these in turn allow the magnitude of the initial integration step to be evaluated. The modelling method is conceptually simple to implement and requires only modest computing facilities. (A Fortran computer code is available to the reader on request from the author.)

Acknowledgments

I am indebted to Dr Hans Hornung for suggesting the above research project and to Dr Frank Houwing for many useful discussions. I am very grateful to Professor John Carver for his support of this project. This project was supported in part by an ARGS grant and an NCAR Visiting Fellowship.

References

Bailey, H. E. (1969). *Phys. Fluids* **12**, 2292.

Ebrahim, N. A., and Hornung, H. G. (1973). *Am. Inst. Aeronaut. Astronaut. J.* **11**, 1369.

Ebrahim, N. A. (1975). Ph.D. Thesis, Australian National University.

Eschenroeder, A. Q., Boyer, D. W., and Hall, J. G. (1962). *Phys. Fluids* **5**, 615.

Garr, L. J., Marrone, P. V., Joss, W. W., and Williams, M. J. (1966). Inviscid nonequilibrium flow behind bow and normal shock waves. Part III: the revised normal shock program. Cornell Aeronautical Lab. Report No. QM-1626-A-12 (III).

Gear, C. W. (1971). *Comm. Ass. Comp. Mach.* **14**, 176.

Hindmarsh, A. C., and Byrne, G. D. (1975). EPISODE: an experimental program for the integration of systems of ordinary differential equations. Lawrence Livermore Lab. Report No. UCID-30112.

Lordi, J. A., Mates, R. E., and Moselle, J. R. (1966). Computer program for the numerical solution of non equilibrium expansions of reacting gas mixtures. Cornell Aeronautical Lab. Report No. NASA CR-472.

McIntosh, M. K. (1971). Ph.D. Thesis, Australian National University.
McRae, G. J., Goodin, W. R., and Seinfeld, J. H. (1982). *J. Comput. Phys.* **45**, 1.
Miller, C. G., and Wilder, S. E. (1976). Tables and charts of equilibrium thermodynamic properties of carbon dioxide for temperatures from 100 K to 25000 K. Langley Research Center Report No. NASA SP-3097.
Newman, P. A., and Allison, D. W. (1966). Direct calculation of specific heats and related thermodynamic properties of arbitrary gas mixtures with tabulated results. Langley Research Center Report No. NASA D-3540.
Stalker, R. J. (1967). *Am. Inst. Aeronaut. Astronaut. J.* **5**, 2160.
Stull, D. R., and Prophet, H. (Eds) (1971). JANAFF thermochemical tables. U.S. National Bureau of Standards Report No. NSRDS-NBS 37.
Treanor, C. E. (1966). *Math. Comp.* **20**, 39.
Vincenti, W. G., and Kruger, C. H. (1977). 'Introduction to Physical Gas Dynamics', 2nd edn (Krieger: New York).
Williams, P. W. (1973). 'Numerical Computation' (Nelson: London).
Zeldovich, V. B., and Raizer, Y. P. (1966). 'Physics of Shock Waves and High Temperature Hydrodynamic Phenomena', Vol. 1 (Academic: New York).

Manuscript received 21 July, accepted 9 December 1983